

Olive Ripening Phase Estimation based on Neural Networks

Marco Mora^{1,3}, Jorge Aliaga³, and Claudio Fredes^{2,3}

¹ Department of Computer Science
Universidad Católica del Maule, Talca, Chile
Department of Agricultural Science
marcomoracofre@gmail.com

² Department of Agricultural Science
Universidad Católica del Maule, Curicó, Chile
cfredes@ucm.cl

³ Laboratory of Technological Research in Pattern Recognition
Universidad Católica del Maule, Talca, Chile
<http://www.litrp.cl>

Abstract. Color of fruits is a relevant parameter to determine ripeness and optimal harvest time. For olives 6 ripening phases based on skin color distribution have been defined. A widely used method by the olive oil and table olives producers is to inspect the olive surface, and estimate the color and ripening phase visually. This method is simple but it is highly subjective and imprecise. This paper proposes a computational method to estimate the color and ripeness of an olive using digital images. A color scale for olives by means of samples of all ripening phases was developed. To represent the olive color, the histogram of the skin color was proposed as a descriptor. To decide the ripening phase, a classifier based on Neural Networks was implemented. The method allows estimating simply and accurately the olive ripening state, which enables to implement it in real production systems.

Keywords: Olive Ripening Phases, Color Histogram, Neural Networks

1 Introduction

The economic activity related to olives is constantly growing and evolving. The introduction of technology in the processing of olives allows improving the quality of the product and to maintain competitiveness against the market requirements. Mainly 2 products are obtained from olives: table olives and olive oil. For table olives, appearance is a relevant feature, given that consumers demand flawless fruits of well-defined size and color. For olive oil, the correct estimation of ripeness by means of color has a direct influence on the quality of the produced oil. To determine a fruit's ripening state, a color scale or color chart are used to estimate the optimal harvest time. The estimation of the color in fruits is performed by visual inspection, or by instruments known as colorimeters. Visual inspection is performed by a human expert; it is a simple and low cost technique,

but it is highly subjective and prone to errors because this judgment varies from person to person. It has little representativeness, given that it is not possible to perform a great amount of analysis and it requires a lot of time. Colorimeters are specialized instruments for measuring color; there are simple and inexpensive colorimeters to measure flat surfaces, and more sophisticated and expensive ones to measure the color of objects.

To address the above problems, a Computer Vision System (CVS) has been developed, featuring digital cameras and images to analyze the fruit's color. In the particular case of olive analysis, the literature presents recent works that adopt techniques of image processing and pattern recognition. In [1] a CVS to discriminate varieties of French olives is developed (Aglандаu, Bouteillan, Lucques, Picholine and Tanche). Pit images (frontal and profile) were used, characteristics such as the histograms of the RGB model and form descriptors (area, perimeter, length, width, etc.) were computed. The classification is performed by Partial Least Squares Discriminant Analysis. The results showed 100% success and concluded that profile images are sufficient for classification. In [2] table olives considering 2 types of images are analyzed. The segmentation is performed on infrared images, and the olives are classified into 5 categories according to the percentage of faulty pixels on the optical image. In [3] a CVS to classify table olives (Manzanilla variety) into 4 categories is presented. Characteristics of the CIE Lab model are used, and the classification is performed by means of a fast algorithm based on Mahalanobis distance. For most of the olive varieties, 6 phases of ripeness are defined. These phases have particular color characteristics. The general sequence of the 6 color states associated with the fruit's ripening evolution is as follows: [4]: green (G), lightgreen (LG), small reddish spots (SRS), turningcolour (TC), purple (P) and black (B). Nevertheless, not all the varieties present the above-mentioned sequence of color characteristic. For the Arbequina variety -one of the varieties of greatest economic interest- the second phase is not lightgreen, but rather greenyellowish [5]. Figure 1 shows Arbequina olives in their different ripening phases. As shown in the figure, for phases 1, 2 and 6 it can be said that there is a predominant color. Nonetheless, for phases 3, 4 and 5 it does not exist a predominant color, and the olives present a set of colors or a color distribution.

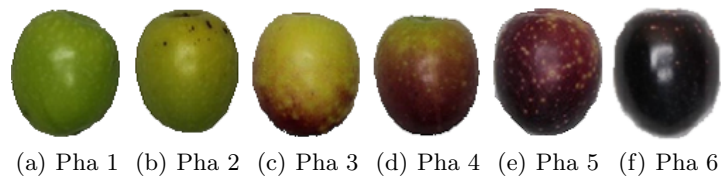


Fig. 1. Arbequina Variety Sequence of Phases

The problem of classifying olives in phases can be resolved in a relatively correct way by a trained person (human expert.) A system that analyzes the

color of the olives by means of digital images must have an adequate representation of the color distribution to get good classification results. This research considers elements that have been validated by the works of literature, such as the use of the CIE Lab color model, and addresses the global problem by using pattern recognition techniques. In addition to the above, the research proposes and validates an original descriptor to represent the olive's color distribution, which consists of the color histogram of the fruit's skin. The pattern recognition system comprises the following stages: Firstly, a color scale based on samples is developed. Secondly, the olive's skin histogram is computed by using the colors of the scale as a basis. Finally, the classification is made by a Multi-Layer Perceptron (MLP), adopting for training an objective methodology to determine the number of neurons in the hidden layer, and avoid model overfitting. The proposed pattern recognition system performs accurately and efficiently the phases classification, obtaining a high rate of success. The characteristics of this method make it suitable for its implementation in reality. For this research, samples of the Arbequina olive -classified by an expert- were used. Besides, MATLAB was used for code development. The article structure is as follows: Section 2 addresses the acquisition and the images segmentation stages. Section 3 explains the process of creating the color scale. In section 4 the proposed descriptor is presented. Then in section 5 the training process of the neural networks is detailed. Section 6 is dedicated to experimentations and results. Finally, in section 7 the research conclusions are presented.

2 Acquisition and Segmentation of Images

2.1 Acquisition of images

Digital images are acquired by means of a system that allows pictures to be taken under constant light conditions. The acquisition system boasts a high resolution digital camera (Canon EOS Rebel T2i) (figure 2 (a)). The camera is held by a support, (figure 2 (b)) to both set up height and avoid shaking when taking the photo. The system also boasts a constant and multidirectional lighting (figure 2 (c)) to diminish as much as possible shadows and highlights in the images. Finally, olives are displayed over a white background (figure 2 (d)) to facilitate their segmenting.

2.2 Segmentation

In spite of the controlled environment, the images present defects that cause problems during segmentation and analysis. The model of color invariant to lighting is adopted [6] because it has been extensively used in image processing since it remains unaffected when there is presence of shadows and highlights ([7], [8]). The expressions of the [6] model are the following:

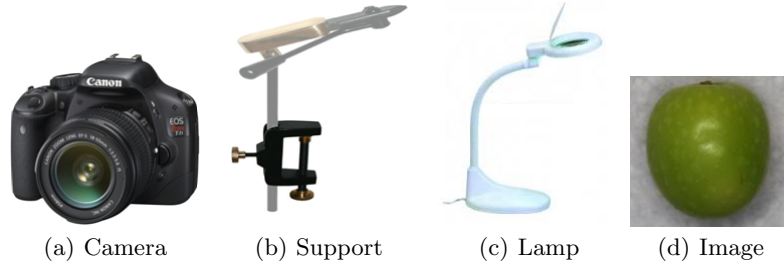


Fig. 2. Acquisition System

$$c_{1i,j} = \arctan \frac{R_{i,j}}{\max(G_{i,j}, B_{i,j})} \quad (1)$$

$$c_{2i,j} = \arctan \frac{G_{i,j}}{\max(R_{i,j}, B_{i,j})} \quad (2)$$

$$c_{3i,j} = \arctan \frac{B_{i,j}}{\max(G_{i,j}, R_{i,j})} \quad (3)$$

where $R_{i,j}$, $G_{i,j}$ y $B_{i,j}$ represent a pixel in the red, green and blue channel of the image. The $c3$ channel is chosen since it offers advantages in the shadow processing in comparison to other channels of the model in [9]. Figure 3 shows the channels of the RGB and $c1c2c3$ models of an olive image. Figure 3(a) shows the original image. Figures 3(b), (c) and (d) correspond to the blue, green, and red channels of the RGB model, respectively. Figures 3(e), (f) and (g) are the $c1$, $c2$ and $c3$ channels of the model invariant to lighting. As seen in the figure, the $c3$ channel features a high contrast between the olive and the background. The background is completely homogeneous, there is no presence of shadows and the highlights on the olive surface are highlighted. The foregoing visually shows that the characteristics of the acquisition system and the use of the $c3$ channel are adequate for the stage of olive segmentation.

For the automatic segmentation of the olive, the widely known Otsu method [10] is adopted. Figure 4 shows in detail the segmentation process. Figure 4(a) shows the original image. The 2 defects mentioned previously are observed. Figure 4(b) shows the binary image resulting from the segmentation by the Otsu method. Figure 4(c) shows the olive pixels resulting from the process of segmentation. As observed in this last image, the segmentation only considers pixels belonging to the olive and discards the pixels affected by the shadow and highlights.

3 Development of the color scale

To represent the olives color, this research proposes as a descriptor the histogram of the fruit's surface. In order to compute the descriptor, it is necessary to create

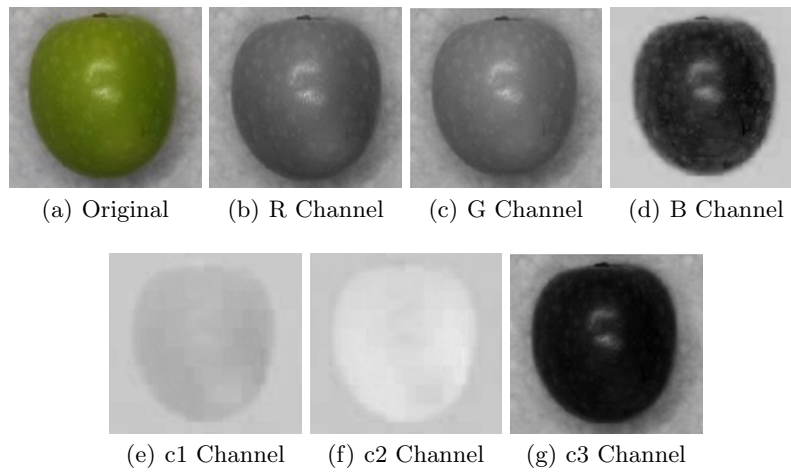


Fig. 3. Channels for RGB and c1c2c3 models

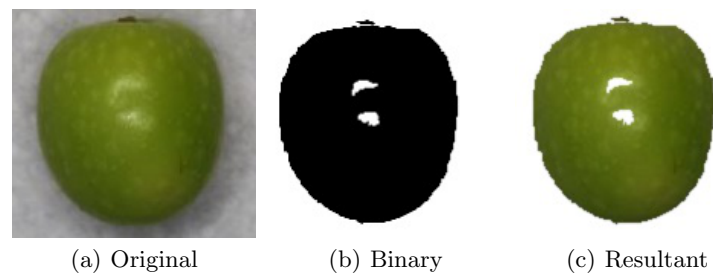


Fig. 4. Images of the segmentation process of the olive

a color scale that represents the olive's ripening evolution. The development of the scale was carried out in the basis of olives samples of the Arbequina variety in different phases (different colors).

For the creation of the scale, olives pixel samples at different ripening stages were considered. Of each of the 6 phases, 5 olives images were taken into account, from which about 50 pixels were selected (250 pixels per phase, 1500 pixels in total). The acquisition of the pixels was conducted using images that had passed through the process of identifying defects, just as described in section 2. For the creation of the scale, exclusively the non repeated pixels were considered, and the CIE Lab coordinates were calculated from those pixels in the basis of the RGB model. The previous process is shown in figure 5, figure 5(a) shows the selection of pixels, and in figure 5(b) the set of samples in the CIE Lab space is presented. It can be appreciated from the three-dimensional graph that the points have a certain tendency or behavior.

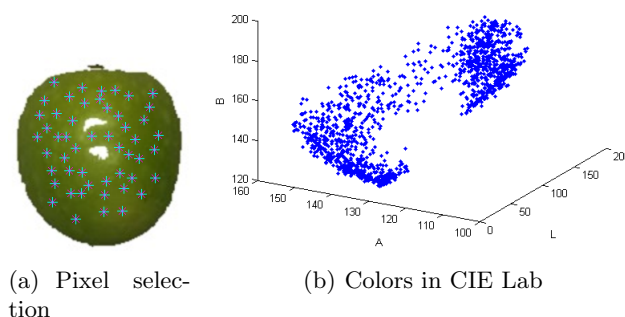


Fig. 5. Olive pixels in CIE Lab model

To explain the behavior of the samples 2 polynomial models whose parameters were estimated by solving an optimization problem that minimizes the Mean Square Error (MSE) based on the Pseudoinverse was used. The first model estimates the coordinate “a” in the basis of “L” of the form $a = F_1(L)$. The second model estimates the coordinate “b” in the basis of “a” and “L” of the form $b = F_2(L, a) = F_2(L, F_1(L))$.

For the estimation of the first model, polynomials of degree 1 until degree 8 were considered. These polynomials have the general form as follows:

$$a = \alpha_0 + \alpha_1 L + \alpha_2 L^2 + \dots + \alpha_n L^n \quad (4)$$

where α_i are the parameters of the equation. The samples graphs and associated polynomials are shown in figure 6.

The equations of the above polynomial are:

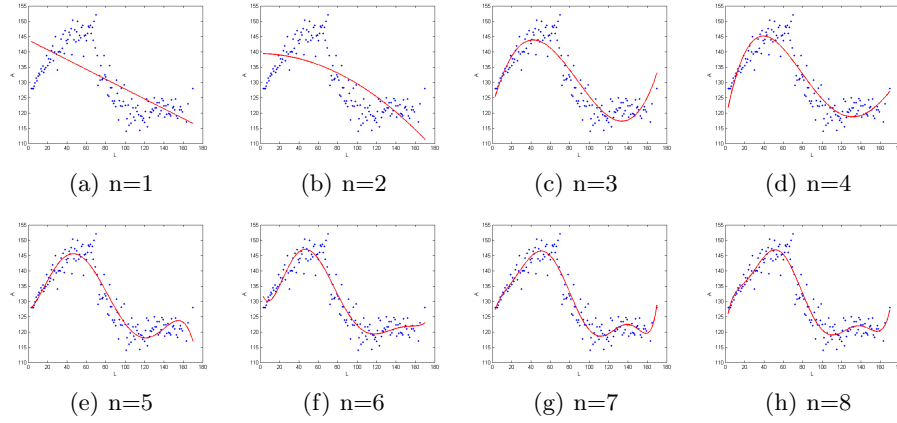


Fig. 6. Polynomials in the plane LA

1. $n=1: a = -0.1606 + 143.8237L$
2. $n=2: a = -0.0009 - 0.0040L + 139.3771L^2$
3. $n=3: a = 0.0001 - 0.0182L + 1.1623L^2 + 121.9604L^3$
4. $n=4: a = 0.0002L - 0.0316L^2 + 1.6837L^3 + 116.9972L^4$
5. $n=5: a = -0.0007L^2 + 0.0248L^3 + 0.2320L^4 + 126.8265L^5$
6. $n=6: a = -0.0025L^3 + 0.1039L^4 - 1.2357L^5 + 134.4069L^6$
7. $n=7: a = -0.0001L^3 + 0.0029L^4 - 0.0702L^5 + 1.2316L^6 + 124.1988L^7$
8. $n=8: a = -0.0001L^4 + 0.0070L^5 - 0.1724L^6 + 2.3843L^7 + 120.2363L^8$

In this case, the polynomial of degree 6 has been chosen to estimate the coordinate “a” in function of “L”, given that it can be seen that this polynomial is that of smaller degree and with less quantity of oscillations to adjust the data.

The second model permits to estimate “b” in function of “L” and “a”. Such model has the following expression:

$$b_i = \beta_0 + \beta_1 L_i + \beta_2 a_i \quad (5)$$

Using the same method to estimate the first model, the resulting polynomial is the following:

$$b_i = 167.4798 + 0.3753L_i - 0.3258a_i \quad (6)$$

To generate the color scale, the previous polynomials are evaluated in the basis of channel “L”. To determine the range of L, the minimum and maximum of the acquired samples were considered (3000 points in the range were considered). The resulting scale is shown in figure 7.

4 Computation of Descriptor for Color Representation

According to the available images, there is a color distribution on the olive. The foregoing indicates that the olive’s color cannot be adequately represented in



Fig. 7. Color scale of the Arbequina olive

the basis of a single color or a representative color. This is the reason why the proposed descriptor corresponds to a histogram of the present colors on the fruit, excluding the defective pixels caused by highlights. It must be noticed that such pixels have been eliminated by the segmentation method.

By using the created color scale, the descriptor to represent the olive's surface color is computed. The proceeding to elaborate the histogram is the following:

- Firstly, the color scale is divided into a segments quantity or bins (in this case, experimentations have been performed with 30 bins).
- As reference color for each bin, the color found at the center of the same one is chosen. So, there exist as many reference colors as bins.
- An olive's image is checked pixel by pixel, and then it is identified to which bin the pixel belongs to by means of the Euclidean distance of the analyzed pixel with respect to the reference color. It is noted that the comparison by Euclidean distance is possible in perceptually correct models of color, so the CIE Lab model is adopted.
- Each element of the histogram accumulates the image pixels belonging to each scale bin

Figure 8 shows the created color scale for the olive, its partitioning into bins, and the reference colors for each one of the segments of the color chart. Table 1 shows the coordinates in the CIE Lab model of the reference colors resulting from each bin.



Fig. 8. Partitioned Histogram

Figure 9 shows examples of the resulting histograms for each one of the 6 ripening phases of the olive. In the histograms of figures 9(a) and (b) a greater presence of yellow and green pixels are perceived, respectively. In the histograms of figures 9(c) and (d) the distribution is relatively uniform, and there is presence of reddish tone pixels. Finally, the histograms of figures 9(e) and (f) present a significant content of dark pixels, particularly the purple and black colors. The

Table 1. Reference Colors per Bin

bin	L	a	b	color	bin	L	a	b	color
1	65,9	-15,9	54,1		16	32,7	1,4	27,7	
2	63,1	-8,8	53,3		17	30,7	4,2	24,8	
3	62,7	-10,5	52,8		18	28,4	7,7	21,5	
4	58,9	-8,5	54,3		19	26,5	10,6	19,1	
5	56,4	-9,1	53,5		20	24,1	13,1	15,7	
6	54,6	-10,4	53,3		21	21,8	15,1	12,8	
7	52,2	-10,9	51,7		22	19,8	16,3	10,7	
8	49,9	-12,5	50,3		23	17,7	17,1	8,4	
9	47,8	-13,1	48,3		24	15,6	16,6	6,8	
10	45,7	-13,1	46,2		25	13,1	15,2	4,6	
11	43,6	-11,5	43,4		26	11,1	13,5	3,7	
12	41,3	-10,5	40,8		27	9,1	10,5	2,9	
13	39,3	-7,9	37,9		28	6,6	7,3	1,3	
14	36,9	-5,2	34,4		29	4,7	3,5	1,2	
15	34,9	-2,4	31,3		30	2,4	1,2	0	

above behavior is consistent with regard to the evolution of the olive's color in the ripening process.

From the point of view of pattern classification, it can be observed that there are 3 groups with well-distinguished histograms: the group formed by the phases 1 and 2, the group formed by the phases 3 and 4, and the group formed by the phases 5 and 6. Likewise, it is appreciated that the histograms of phases of the same group are similar among them, which implies the need of a supervised learning method to differentiate them.

5 Estimation of the ripening phase by means of classification

As it was previously commented, the need to differentiate the 6 phases -on the part of olive oil and table olives producers- implies a supervised learning strategy to create the classifier. In this case, a Multilayer Perceptron is proposed due to its easiness to adjust the classification error to a desired level, and to differentiate the similar classes. For the creation and validation of the classifier a total of 202 images were used. From this total, 67% (132 images) were used for the training set and 33% (70 images) were used for the test set. An expert classified the samples in its different phases. Table 2 shows the detail of the number of samples per set and per phase.

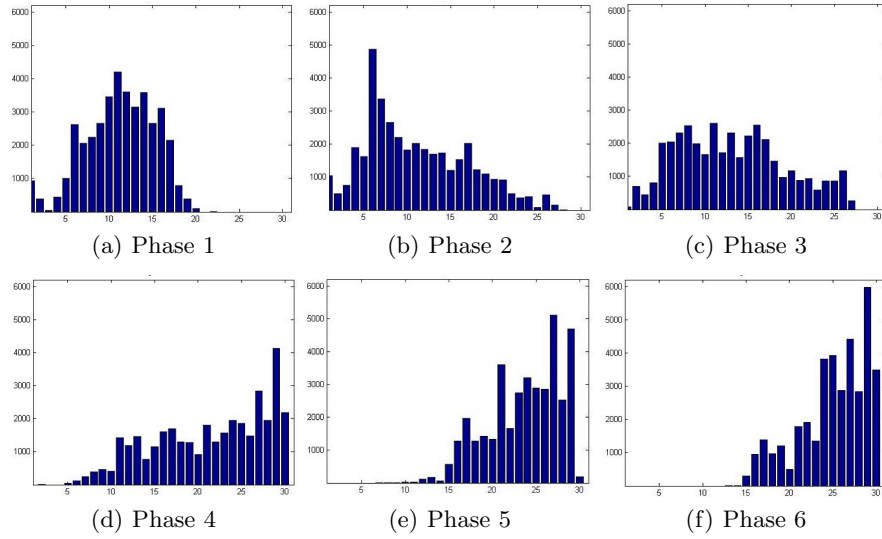


Fig. 9. Histograms per ripening phase

Table 2. Samples per phase

Phase	# Images		Total
	Training Set	Test Set	
1	32	16	48
2	16	9	25
3	25	13	38
4	22	12	44
5	19	10	29
6	18	10	28
Total	132	70	202

A MultiLayer Perceptron (MLP) network is used, since it is a universal approximator of functions and it is widely used in tasks of pattern classification. Figure 10 shows the structure of the Multilayer Perceptron. The quantity of neurons of the input layer has to do with the number of elements that make up the descriptor. It has an output neuron that indicates the belonging or not belonging to a specific class. The quantity of neurons of the hidden layer is a parameter to be defined in the process of network training, having the need of having the smaller quantity of neurons in such layer to assure a good generalization of the network.

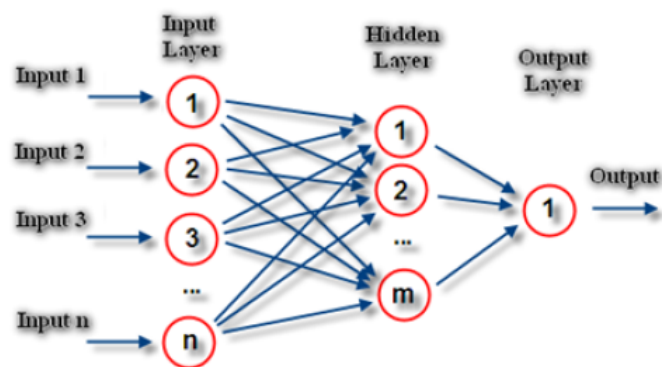


Fig. 10. Multi-Layer Perceptron

The structure and functioning of the classifier is as follows:

- It is composed by 6 MLP neural networks, one per ripening phase.
- Each MLP has 30 inputs, given that the histogram has 30 bins.
- Each MLP has 1 output, so that every network decides the belonging of the pattern to a phase.
- The histograms of every olive are classified by the 6 networks. The olive's phase corresponds to the network whose output is closer to 1.

The objective of the training process is to determine the weights of every network, and also to determine the number of neurons in the hidden layer of every network. The characteristics of such process are discussed below:

- Every MLP was trained with a Levenberg-Marquardt Algorithm, since they have a better convergence speed than the Steepest Descent used by the Backpropagation algorithm.

- For each network training, the initial weights were randomly chosen. This is intended to avoid local minima error.
- For each training, the elements of the training and test set were randomly chosen, as a means of finding a representative training set of the sample universe.
- The training methodology consists of gradually raising the number of neurons of the hidden layer, starting with one neuron. For each quantity of neurons of the hidden layer it is proceeded to train the network a large number of times (1000 trainings in this case, approximately). The network with the best average of success -considering the training and test set- is chosen. It was also considered that the network must have more than 95% of success in the Training set, and more than 90% of success in the Test set.
- As the quantity of neurons rises in the hidden layer, the averages of success also improve. Nonetheless, there is a moment when these averages stabilize and don't improve significantly. The network of smaller quantity of neurons is chosen when the phenomenon of error stabilization starts. It is to notice that to have a network of a low quantity of neurons in the hidden layer is desired to have a better network generalization, and for the classifier to have the simplest possible architecture.
- Once determined the quantity of neurons of the hidden layer, a large amount of trainings are performed one more time to find the best network with that quantity of neurons with best average of success (100000 trainings were performed in this case).

The advantage of the methodology used for training is that it can be automated, and classifiers with a low percentage of error and a good generalization can be found thanks to it.

6 Results

Table 3 shows the result of the process of training, detailing the number of neurons found in the hidden layer and the percentages of error of the best network found for each one of the phases. From this table it can be observed that the number of neurons in the hidden layer is low, which implies an architecture of the classifier adapted to real implementations and that permits a good generalization against unknown samples. It is observed that the percentages of success in both the training and test set are high (above 90%), showing that the proposed color descriptor can differentiate the ripening phases adequately.

Table 3 gives information about the individual behavior of each network, and not about the classifier in its set. Table 4 is presented to obtain information about the global performance of the classifier. This table is created by classifying all the existing patterns, presenting each pattern to the 6 networks simultaneously. The phase of the pattern is decided by considering which network's output is closer to 1. The content of the table is interpreted as follows: Observing the first row, it can be seen that there is a total of 48 samples of the phase 1 (100%) of which

Table 3. Training of the Neural Classifier

Network	# Neurons Hidden Layer	Hit % Training Set	Hit % Test Set
Network Phase 1	3	96,21	90,00
Network Phase 2	3	96,97	90,00
Network Phase 3	2	96,21	95,71
Network Phase 4	2	95,46	92,86
Network Phase 5	1	96,97	94,29
Network Phase 6	1	97,73	98,57

46 (96%) were classified correctly, and 2 (4%) were assigned to other classes. All the other rows are interpreted in the same way. From this table analysis it can be concluded that the proposed descriptor explains adequately the olive's ripening phenomenon.

Table 4. Global Results of Classification

Red	Hit		Error	
	Total	Number	Number	Hit% Error%
Red Fase 1	48	46	2	96 % 4 %
Red Fase 2	25	18	2	92 % 8 %
Red Fase 3	38	36	2	95 % 5 %
Red Fase 4	34	32	2	94 % 6 %
Red Fase 5	29	27	2	93 % 7 %
Red Fase 6	28	27	1	96 % 4 %
Total	202	191	11	95 % 5 %

7 Conclusion

This research has been proposed as an original method to estimate the olive's ripeness based on pattern recognition techniques and image treatment. This research proposes a histogram of the olive's surface colors as a descriptor to identify the fruit's ripening phases. The creation of this histogram was carried out by means of a color scale based on samples of olives in different phases. A classifier was methodologically designed based on neural networks to determine the phase of the olive. The results of classification show a high Hit Rate, which indicates that the proposed descriptor allows identifying adequately the olive's ripening phases. The characteristics of the developed method allow automating a process that at present is carried out in visual form. Of these results it can be said that this method responds adequately to the current need of olive oil and table olives producers to estimate the ripening phases of the olive and to decide the time of harvest.

Acknowledgment

This research is financed by the research project FONDEF IDEA en 2 Etapas ID15i10142 2015 “Estimación del Contenido de Aceite en Olivas en base a Tecnologías no Destructivas” (Estimation of Olive Oil Content based on Non Destructive Technologies), Scientific and Technological Development Support Fund (FONDEF), National Commission for Scientific and Technological Research (CONICYT), Government of Chile.

References

1. Vanloot, P., Bertrand, D., Pinatel, C., Artaud, J., Dupuy, N.: Artificial vision and chemometrics analyses of olive stones for varietal identification of five french cultivars. *Computers and Electronics in Agriculture* **102** (2014) 98–105
2. Guzmán, E., Baeten, V., Pierna, J.A.F., García-Mesa, J.A.: Infrared machine vision system for the automatic detection of olive fruit quality. *Talanta* **116** (2013) 894–898
3. Diaz, R., Faus, G., Blasco, M., Blasco, J., Molto, E.: The application of a fast algorithm for the classification of olives by machine vision. *Food research international* **33** (2000) 305–309
4. Loudiyi, W., Chmitah, M., Loussert, R., Mahhou, A., Boulouha, B.: Morphologic and physiologic characters of olive clones from picholine marroqui variety. *Olivae* **3** (1984) 26–31
5. Criado, M., Motilva, M., Goñi, M., Romero, M.: Comparative study of the effect of the maturation process of the olive fruit on the chlorophyll and carotenoid fractions of drupes and virgin oils from arbequina and farga cultivars. *Food chemistry* **100** (2007) 748–755
6. Gevers, T., Smeulders, A.W.: Color-based Object Recognition. *Pattern Recognition* **32** (1999) 453 – 464
7. Salvador, E., Cavallaro, A., Ebrahimi, T.: Shadow identification and classification using invariant color models. In: *Acoustics, Speech, and Signal Processing, 2001. Proceedings.(ICASSP'01). 2001 IEEE International Conference on.* Volume 3., IEEE (2001) 1545–1548
8. Salvador, E., Cavallaro, A., Ebrahimi, T.: Cast shadow segmentation using invariant color features. *Computer vision and image understanding* **95** (2004) 238–259
9. Avila, F., Mora, M., Fredes, C., Gonzalez, P.: Shadow Detection in Complex Images Using Neural Networks: Application to Wine Grape Seed Segmentation. In: *Adaptive and Natural Computing Algorithms.* Volume 7824 of *Lecture Notes in Computer Science.* Elsevier (2013) 495–503
10. Otsu, N.: A threshold selection method from gray-level histograms. *Automatica* **11** (1975) 23–27